

Article

Effects of Temperature on the Tribological Properties of Cylinder-Liner Piston Ring Lubricated with Different Oils

Chang Du ^{1,2}, Chenxing Sheng ^{1,2,*}, Xingxin Liang ^{1,2,*}, Xiang Rao ^{1,2} and Zhiwei Guo ^{2,3} 

¹ School of Naval Architecture Ocean and Energy Power Engineering, Wuhan University of Technology, Wuhan 430063, China

² Reliability Engineering Institute, National Engineering Research Center for Water Transportation Safety, Wuhan 430063, China

³ School of Transportation and Logistics Engineering, Wuhan University of Technology, Wuhan 430063, China

* Correspondence: scx01@126.com (C.S.); xingxin@whut.edu.cn (X.L.); Tel.: +86-18672988909 (C.S.); Tel.: +86-15972971898 (X.L.)

Abstract: As one of the important friction pairs of a diesel engine, the cylinder-liner piston ring (CL-PR) faces a harsh high-temperature working environment. To explore the mapping relationship between the friction performance of the CL-PR and the change in temperature, the reciprocating-friction and wear-testing machine was used to analyze the friction performance and lubrication performance of four kinds of lubricating oil at different temperatures (room temperature, 60 °C, 90 °C, and 120 °C) from the friction coefficient, contact resistance and surface topography. The results show that the tribological properties of the four lubricating oils show different trends with the increase in temperature. The friction coefficient of the base oil first decreases and then increases with the increase in temperature; this shows that the friction property of the base oil is improved by a certain temperature rise, and the increase in temperature promotes the formation of an oxide film and reduces the friction coefficient. While the friction coefficient of other three lubricating oils with specific application scenarios increases first and then remains stable, the wear of the friction pair is the most severe at 120 °C. The wear forms are abrasive wear and adhesive wear.

Keywords: cylinder-liner piston ring; temperature; tribological property; lubrication characteristics



Citation: Du, C.; Sheng, C.; Liang, X.; Rao, X.; Guo, Z. Effects of

Temperature on the Tribological Properties of Cylinder-Liner Piston Ring Lubricated with Different Oils.

Lubricants **2023**, *11*, 115. <https://doi.org/10.3390/lubricants11030115>

Received: 6 February 2023

Revised: 20 February 2023

Accepted: 4 March 2023

Published: 6 March 2023



Copyright: © 2023 by the authors. Licensee MDPI, Basel, Switzerland. This article is an open access article distributed under the terms and conditions of the Creative Commons Attribution (CC BY) license (<https://creativecommons.org/licenses/by/4.0/>).

1. Introduction

In response to global environmental pollution and the energy-shortage problem, the International Maritime Organization (IMO) has introduced new requirements for both the Energy Efficiency Existing ship Index (EEXI) process and the Energy Efficiency Design Index (EEDI), and new-energy ships have become one of the main development directions for ships [1–4]. In addition, as more and more countries regard “carbon neutrality” as an important development goal, LNG ships usher in broad development prospects with an excellent environmental performance, which can be seen from the fact that nearly 30% of new ship orders in 2021 were powered by LNG fuel, setting a record [5,6]. However, although LNG fuel has a huge resource reserve and excellent cleaning performance compared with diesel fuel, it also increases its in-cylinder combustion temperature [7–9]. It also means that the cylinder-liner piston ring (CL-PR) faces a harsher working environment, such as higher temperature; as one of the important factors affecting the working performance of the CL-PR friction pair of a diesel engine, temperature not only has a great influence on the friction performance of the CL-PR, but also affects the reliability and economy of the diesel engine [10–13]. Specifically, temperature has a great influence on the structure of the friction surface, the viscosity of the lubricating oil and the thickness of the lubricating film [14–16]. High temperature will also affect the lubricating performance of the lubricating oil, and high temperature may promote the reaction between the metal on the surface of the friction pair and the oxygen, forming an oxide film [17,18]. In summary,

temperature and lubricating-oil viscosity will both affect the friction performance of the CL-PR. Therefore, exploring the effects of temperature on the tribological properties of the CL-PR lubricated with different oils has great significance for the further development of LNG engines.

In recent years, many researchers have studied the effect of temperature on friction properties. Yi C.X. [19] et al. investigated the temperature and heat-partitioning coefficient during friction between polymer and steel, and some factors affecting friction temperature and heat-partitioning coefficient were analyzed by experiment and simulation. Sepehr S. [20] et al. studied the elevated-temperature contact creep and friction of nickel-based superalloys by machine-learning assisted finite-element analysis, and found that increasing temperature and dwell time will lead to a friction-coefficient increase, yet the dominance of dwell time effects the reduction at a higher temperature and load. Ye L.X. [21] et al. analyzed the friction and wear behavior of copper-metal matrix composites at temperatures up to 800 °C, and the results show that the friction coefficient presents different trends in different temperature ranges. In addition, in view of the harsh temperature condition faced by the CL-PR, many scholars have also analyzed the influence of temperature on the CL-PR. For example, Caglar D. [22] et al. studied the effect of energy-efficiency enhancement of controlled cylinder-liner temperature in a marine diesel engine using the model-analysis approach, and the result shows that the controlled cylinder-wall temperature could be considered as one of the methods to solve the efficiency and emission problem in ships in the near future. Hubert K. [23] et al. reported the effect of temperature on the tribological properties of 1-butanol-diesel fuel blends, and analyzed the lubricating-properties transformation law of different 1-butanol volume fractions in the 1-BDF under different temperatures.

Numerous studies have confirmed that both temperature and lubricating oil affect the friction performance of the friction pair. For diesel engines, the high-temperature operating condition of the CL-PR and the lubricating performance of the lubricating oil are also important factors that affect the working efficiency of the diesel engine. Although a lot of research has been carried out on the effect of temperature or lubricating oil on the friction characteristics of CL-PR, the research studies on the effects of temperature on the tribological properties of CL-PR lubricated with different oils are relatively small in number, and the influence mechanism of lubricating oil on the friction characteristics of CL-PR at a high temperature is still uncertain. In this paper, a controlled trial was designed for a reciprocating-friction and wear tester to explore the influence mechanism of different lubricating oils on the friction performance of CL-PR at a high temperature, which has great significance for the sustainable development of diesel engines towards higher in-cylinder-combustion temperatures and a higher working efficiency.

2. Materials and Methods

2.1. Materials Preparation

In order to explore the effect of different temperatures on friction characteristics under different lubricating oils, four different oils were selected to study the variation law of friction performance of CL-PR under different temperature conditions. Lubricant A (70 N base oil) is a base oil without other additives, lubricant B (Mobil 15w-40) is suitable for vehicle LNG-fuel engine lubrication, lubricant C (Sinopec T200 15w-40) is commonly used for lubricating diesel engines for vehicles, and lubricant D was selected from the cylinder oil used in the in-service ships (5040 Marine cylinder oil). The lubricating oils used in the test are shown in Figure 1; Table 1 describes the basic parameters.

In addition, the viscosity–temperature characteristics of four kinds of lubricating oil at test temperature were measured by rheometer to further characterize the difference between the four lubricating oils, which can help analyze the influence mechanism of the lubricating oil on the friction characteristics of the friction pair. In addition, the viscosity–temperature curves of four kinds of lubricating oils in the range of 20–130 °C measured by rheometer under 20 N shear force are shown in Figure 2. The test sample was made of S195 single-cylinder diesel-engine cylinder liner, cut into 120 mm × 80 mm specimens; the

material is wear-resistant alloy cast iron, the piston-ring slices correspond to the size of the cylinder-liner sample, and the material is ductile iron, as shown in Figure 3. The amount of lubricating oil used during the test was 15 mL/h, which was calculated according to the equivalent of the cylinder oil consumption of the in-service ship. Since there was no consumption of lubricating oil during the test, the friction pair was always surrounded by excess lubricating oil, so it is considered that the exact amount of lubricating oil used was irrelevant for the test result.



Figure 1. Four types of lubricating oil.

Table 1. Basic parameters of the four lubricating oils.

Lubricant	Viscosity at 40 °C	Viscosity at 100 °C	Viscosity Index	Flash Point	Pour Point
Lubricant A	15.3 mPa.s	3.6 mPa.s	99	210 °C	−15 °C
Lubricant B	96.2 mPa.s	10.1 mPa.s	151	243 °C	−36 °C
Lubricant C	115.1 mPa.s	13.2 mPa.s	101	225 °C	−27 °C
Lubricant D	174.4 mPa.s	17.5 mPa.s	105	274 °C	−12 °C

2.2. Tribological Tests and Characterizations

The friction tests involved in this paper were all completed on the reciprocating-friction and wear-testing machine. The schematic diagram of the testing machine is shown in Figure 4: the cylinder-liner sample and piston-ring sample are fixed in the corresponding molds, and the temperature conditions during the test were provided by the ceramic heating plate and the thermostat. The schematic diagram of the fixture is shown in Figure 5. During the test, the friction force and pressure were collected in real time by the corresponding sensors, to evaluate the friction characteristics of the friction pair.

In addition, a constant voltage was applied to the CL-PR, due to the great difference in electrical conductivity between the lubricating oil and the metal; when the thickness of the lubricating-oil film changes, the contact resistance between the friction pairs will change accordingly. In addition, it should be noted that the effect of temperature on the electrical conductivity of the four lubricating oils and the sample can be ignored, so the change in the thickness of the lubricating-oil film of the friction pair can be qualitatively analyzed by the change in contact resistance.

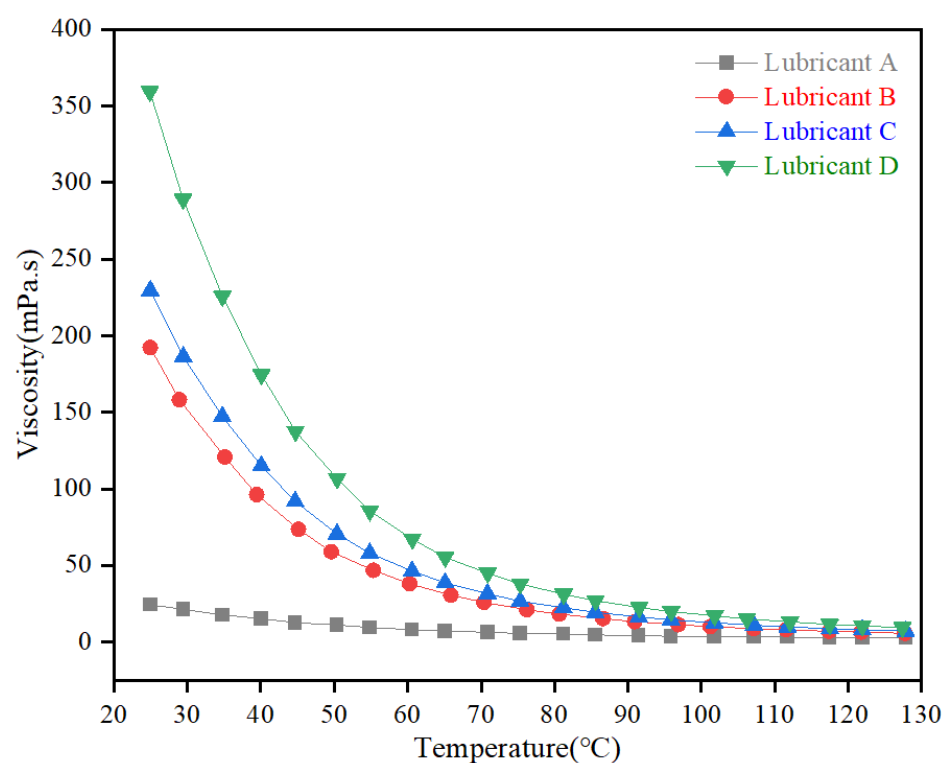


Figure 2. Four kinds of lubricating-oil viscosity–temperature curve.

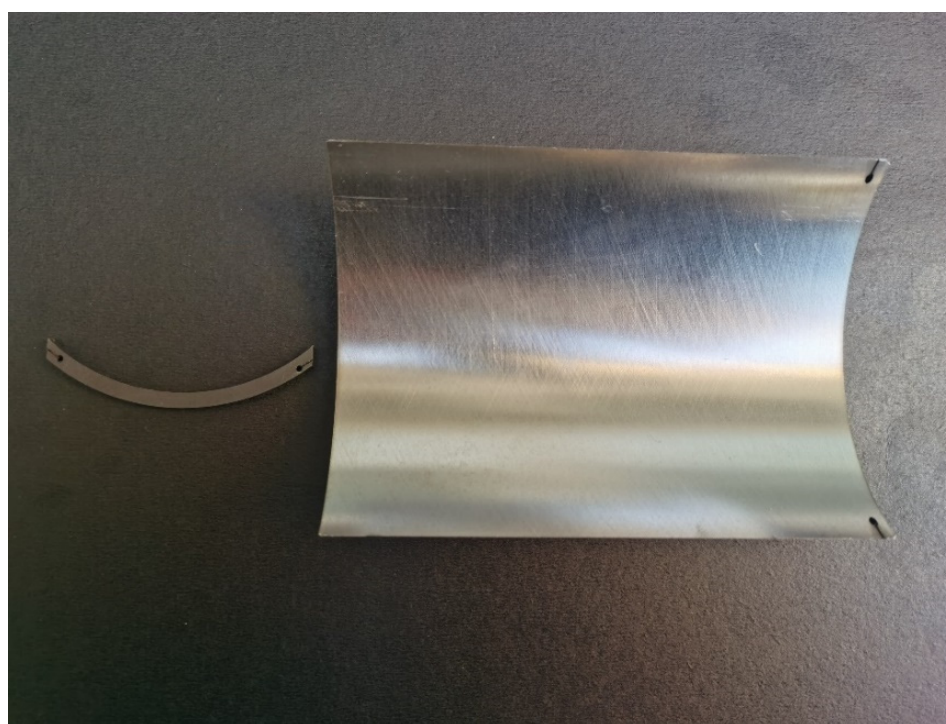


Figure 3. Cylinder-liner piston-ring sample.

Finally, the friction surface of the cylinder-liner sample was analyzed using the 3D surface profilometer (HUST, Wuhan, China) and the scanning electron microscope (SEM, Tescan, Brno, Czech). Before the friction test and the surface-topography measurement, the surface of the cylinder-liner samples was wiped with alcohol, to eliminate the interference of other factors. To prevent accidental factors affecting the results, the sampling range of

the profiler was $0.8 \text{ mm} \times 0.8 \text{ mm}$, and each cylinder liner collected four sample points and took the average value.

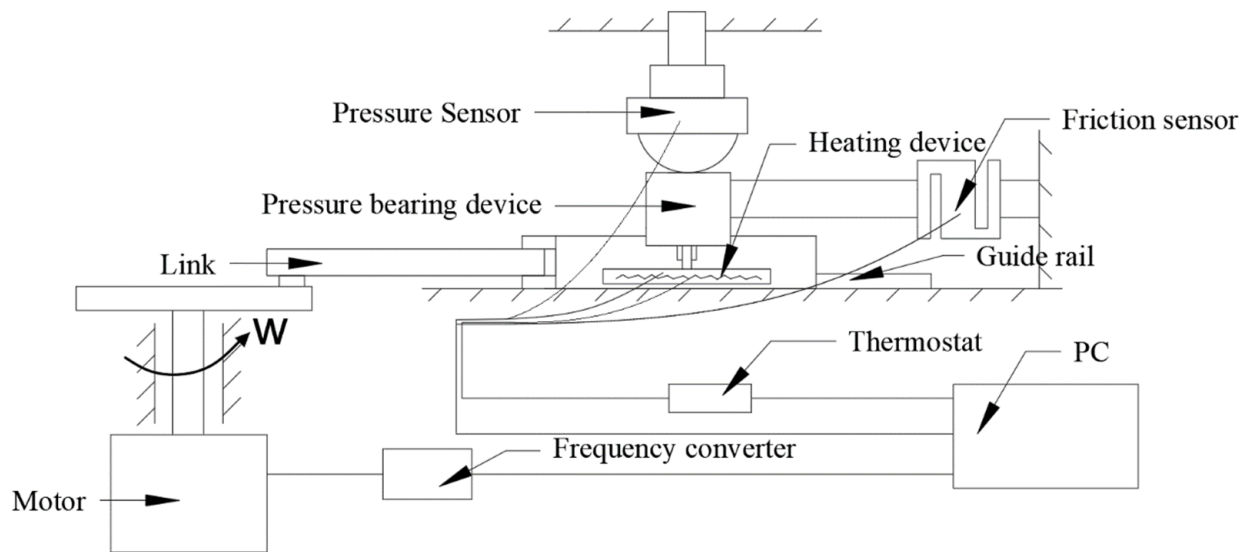


Figure 4. Reciprocating-friction and wear tester.

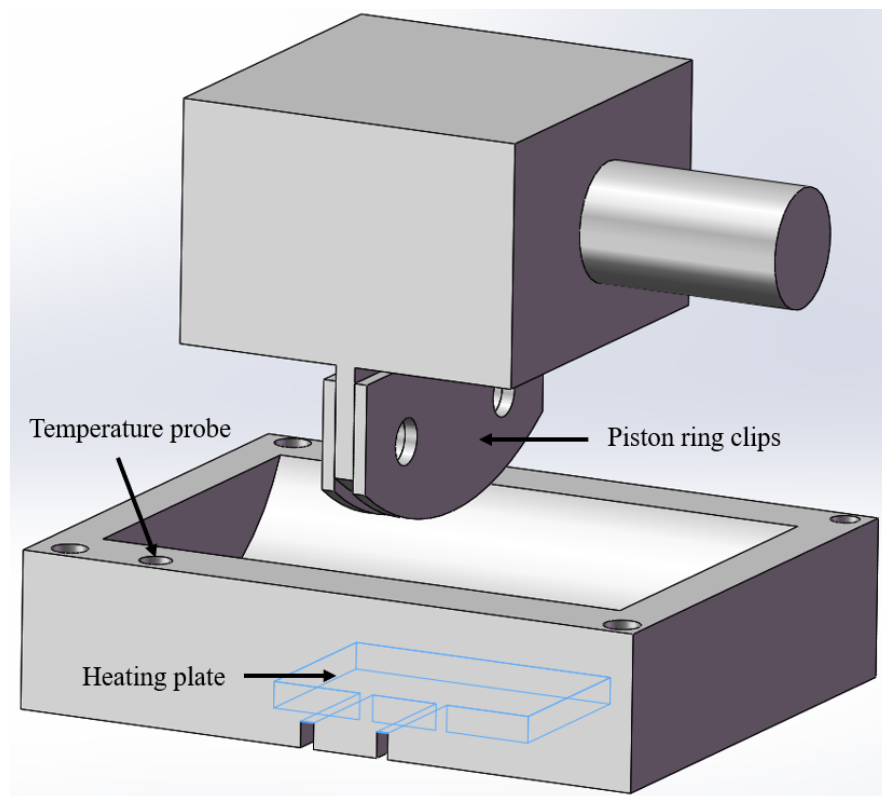


Figure 5. Schematic diagram of CL-PR mold.

2.3. Experimental Method

For the low-speed and heavy-load operating conditions of large ships, the load and speed of the test conditions were determined to be 300 N and 100 r/min, respectively. The four temperature conditions were room temperature, 60 °C, 90 °C and 120 °C. The tribological properties of the four lubricating oils at different temperatures were studied by the friction- and wear-testing machine. The test arrangement is shown in Table 2.

Table 2. Experimental design.

Lubricant Oil	Test Condition	Temperature
Lubricant A	300 N–100 r/min	room temperature, 60 °C, 90 °C, 120 °C
Lubricant B	300 N–100 r/min	room temperature, 60 °C, 90 °C, 120 °C
Lubricant C	300 N–100 r/min	room temperature, 60 °C, 90 °C, 120 °C
Lubricant D	300 N–100 r/min	room temperature, 60 °C, 90 °C, 120 °C

During the test, 30 mL base oil was evenly added between the friction pairs. The lubrication method was drip-oil lubrication, and the test time for each group was 2 h.

3. Results

The test results show that the temperature and lubricating oil have different degrees of influence on the friction performance and lubrication characteristics of the CL-PR friction pair. In this paper, the friction state of the friction pair under different test conditions was analyzed in three aspects: friction coefficient, contact resistance and surface topography of the friction pair.

3.1. Friction Coefficient

The average friction coefficients of the four lubricating oils at different temperatures are shown in Figure 6 and Table 3. From the figure, the friction properties of the four lubricating oils show different changes in trend with the increase in temperature. With the increase in temperature, the friction coefficient of base oil A decreased first and then increased, and the minimum friction coefficient appeared at 60 °C, while the friction coefficient of other three kinds of lubricating oil all increased first and then maintained a stable level, with the lowest friction coefficient appearing at room temperature. Compared with the other three lubricating oils, the friction coefficient of base oil A was largest under all temperature conditions, which also fully demonstrated the importance of lubricating-oil additives for the tribological properties of friction pairs under complex and harsh working conditions.

For base oil A, the increase in temperature had a positive promoting effect on the friction pair of CL-PR. With the increase in temperature, the viscosity of the lubricating oil decreased, the viscous resistance decreased, and the friction coefficient of the friction pair was reduced. In addition, the temperature increase promoted the oxidation reaction of the metal interface between the friction pair, and the oxidation film generated on the friction surface also improved the friction characteristics of the friction pair [24,25]. Therefore, the friction coefficient of base oil A was lower than at room temperature when the temperature condition was 60 °C and 90 °C, indicating that the friction performance at the two temperature conditions was better than at room temperature. In addition, the friction coefficient reached the maximum when the temperature was 120 °C, indicating that as the temperature continued to rise, the friction property deteriorated. With the further increase in temperature, the adhesion point of the friction surface increased, increasing the friction coefficient. It should be noted that, at the end of the test at 120 °C, a small amount of black adhesive substance was observed on the surface of the cylinder liner. Since the temperature had exceeded the effective working temperature of base oil A, the lubricating oil slightly carbonized and mixed with the grinding chips, to form the black adhesive substance which led to the deterioration of the friction performance of base oil A at 120 °C. For the other three lubricating oils, the lowest friction coefficients all appeared at room temperature, indicating that the temperature increase decreased the friction property of the friction pair. For lubricating oil B, the friction coefficient at 60 °C was 0.1004, which was 16.37% higher than at room temperature, and the friction coefficient at 120 °C was 0.1034, which was only 2.9% higher than 60 °C. This indicated that, with the continuous increase in temperature, the friction property does not change significantly within the temperature range of 60 °C to 120 °C, and the friction coefficient was kept at a stable level.

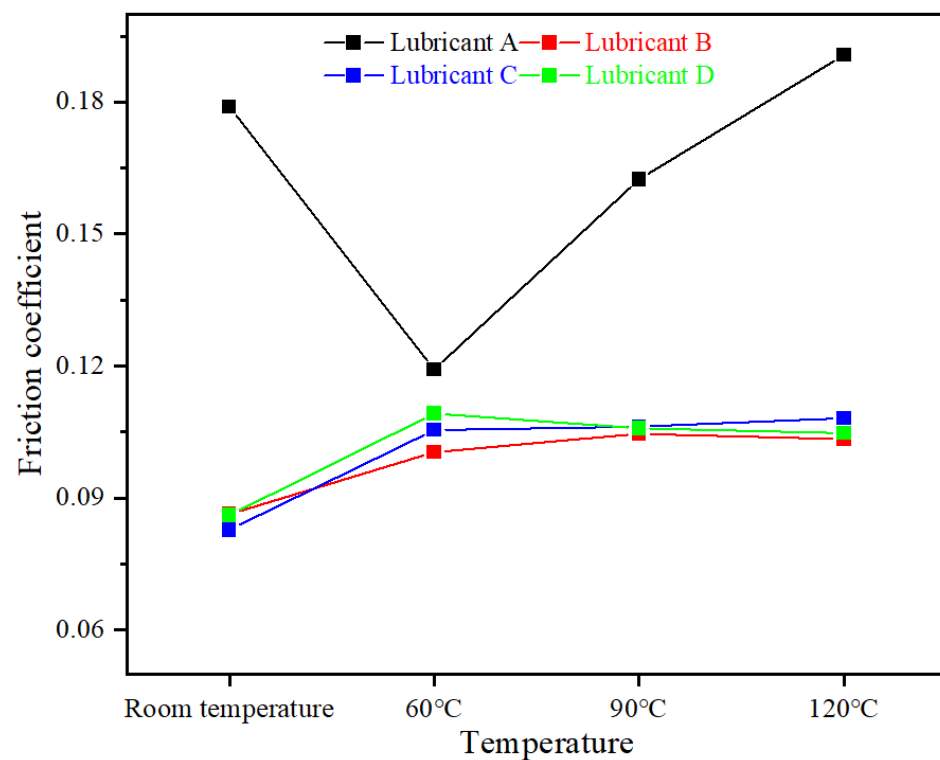


Figure 6. The average coefficient of friction of the four temperatures.

Table 3. The average coefficient of friction of the four temperatures.

	Lubricant A	Lubricant B	Lubricant C	Lubricant D
Room temperature	0.1789	0.0863	0.0828	0.0861
60 °C	0.1192	0.1004	0.1054	0.1092
90 °C	0.1624	0.1045	0.1062	0.1058
120 °C	0.1907	0.1034	0.1081	0.1047

Similarly, lubricating oil C and lubricating oil D also showed the same change trend. Compared with room temperature, the friction coefficient of lubricating oil C and lubricating oil D increased by 27.29% and 26.83%, respectively, at 60 °C. Compared with 60 °C, the friction coefficient of lubricating oil C and lubricating oil D changed by 2.5% and 4.1%, respectively, at 120 °C. As can be seen from Figure 2, compared with base oil A, the viscosity of the three lubricating oils at room temperature was much higher than that of the base oil, and the viscosity of lubricating oils B, C, and D decreased significantly with the increase in temperature. As an important index for measuring the lubricating-oil lubrication characteristic, although the decrease in viscosity leads to the decrease in the internal viscous resistance of lubricating oil, but the film-forming ability of the lubricating oil is also greatly reduced with the decrease in viscosity; This directly affects the thickness of the lubricating-oil film between the friction pairs, thus increasing the friction coefficient and reducing the friction performance. In addition, in the range from room temperature to 60 °C, the viscosity of the three lubricating oils decreased significantly, while in the range from 60 °C to 120 °C, although the viscosity of the lubricating oil still decreased with the temperature increase, compared with conditions lower than 60 °C, the viscosity decreased slightly. This was an important reason why the friction coefficient of the lubricating oils B, C, and D remained stable within the temperature range of 60 °C to 120 °C.

The change trend of the friction coefficient of the four lubricating oils over time is shown in Figure 7. Compared with the base oil, the friction-coefficient trend of lubricating oils B, C, D was more stable at room temperature. At room-temperature condition, the three lubricating oils all showed better anti-friction and anti-wear performance, and the

friction-coefficient fluctuation mainly occurred in the first half hour of the test, when the sample was still in the run-in period and the frictional property was not very stable. Compared with the variation trend of the friction coefficient at room temperature, the friction coefficient fluctuated significantly with the increase in temperature, which was because the increase of temperature led to the intensification of the wear of the friction pair, thus causing the fluctuation in the friction coefficient.

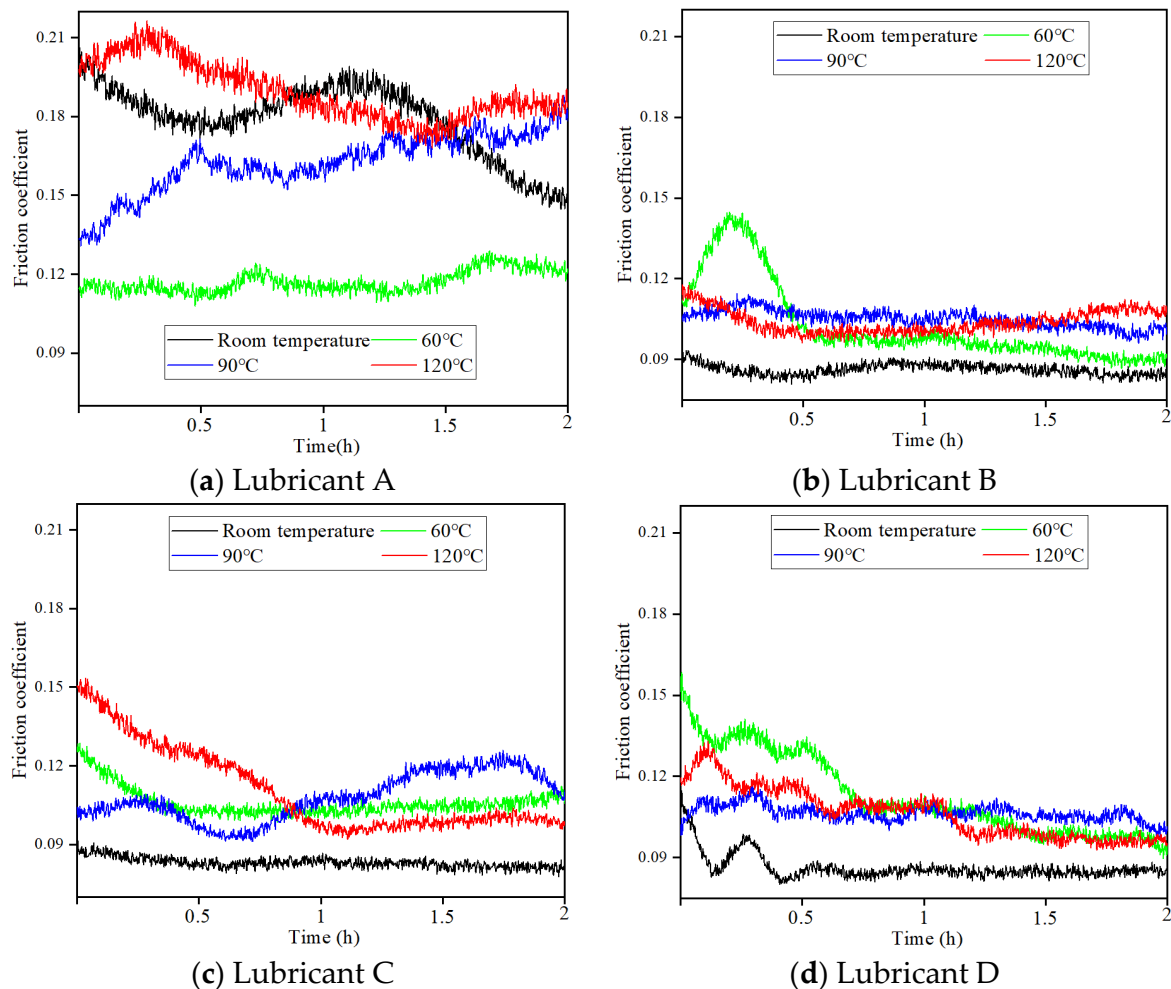


Figure 7. (a) Variation trend of friction coefficient over time, of lubricant A; (b) variation trend of friction coefficient over time, of lubricant B; (c) variation trend of friction coefficient over time, of lubricant C; (d) variation trend of friction coefficient over time, of lubricant D.

3.2. Contact Resistance

As shown in Figure 8 and Table 4, the contact resistance of the four lubricating oils varied greatly and showed different trends at different temperatures, indicating that temperature has a great influence on the lubrication state of the four lubricating oils. From Figure 8, it can be seen that the contact resistance of base oil A firstly increased and then decreased with the increase in temperature, which corresponded to the change in the law of friction coefficient. This indicated that the lubrication state of the friction pair was improved by the increase in temperature, and that it formed a thicker lubricating oil film. The maximum value was reached at 60 °C, and the friction coefficient was also the lowest at this time. As the temperature continued to rise, the contact resistance became smaller at 90 °C, indicated that the film-forming ability of the lubricating oil decreased, due to the rise in temperature, and the thickness of the lubricating-oil film which formed was smaller than at room-temperature condition. However, the friction coefficient at this condition was lower than that at room temperature, indicating that although the lubrication state of the friction

pair was lower than at room temperature, the oxidation film generated by the increase in temperature alleviated the friction between the friction pairs, so the friction performance was still better than at room temperature. As the temperature continued to rise, the friction coefficient reached the maximum value of 120 °C, and the contact resistance was at the minimum value, showing that the thickness of the lubricating-oil film was at the minimum. Combined with the analysis of the friction coefficient, the lubrication performance of base oil A deteriorated, due to the high temperature, and the lubricating oil carbonized and mixed with abrasive particles, aggravating the wear on the friction surface. This result in the worst friction performance of CL-PR, at 120 °C.

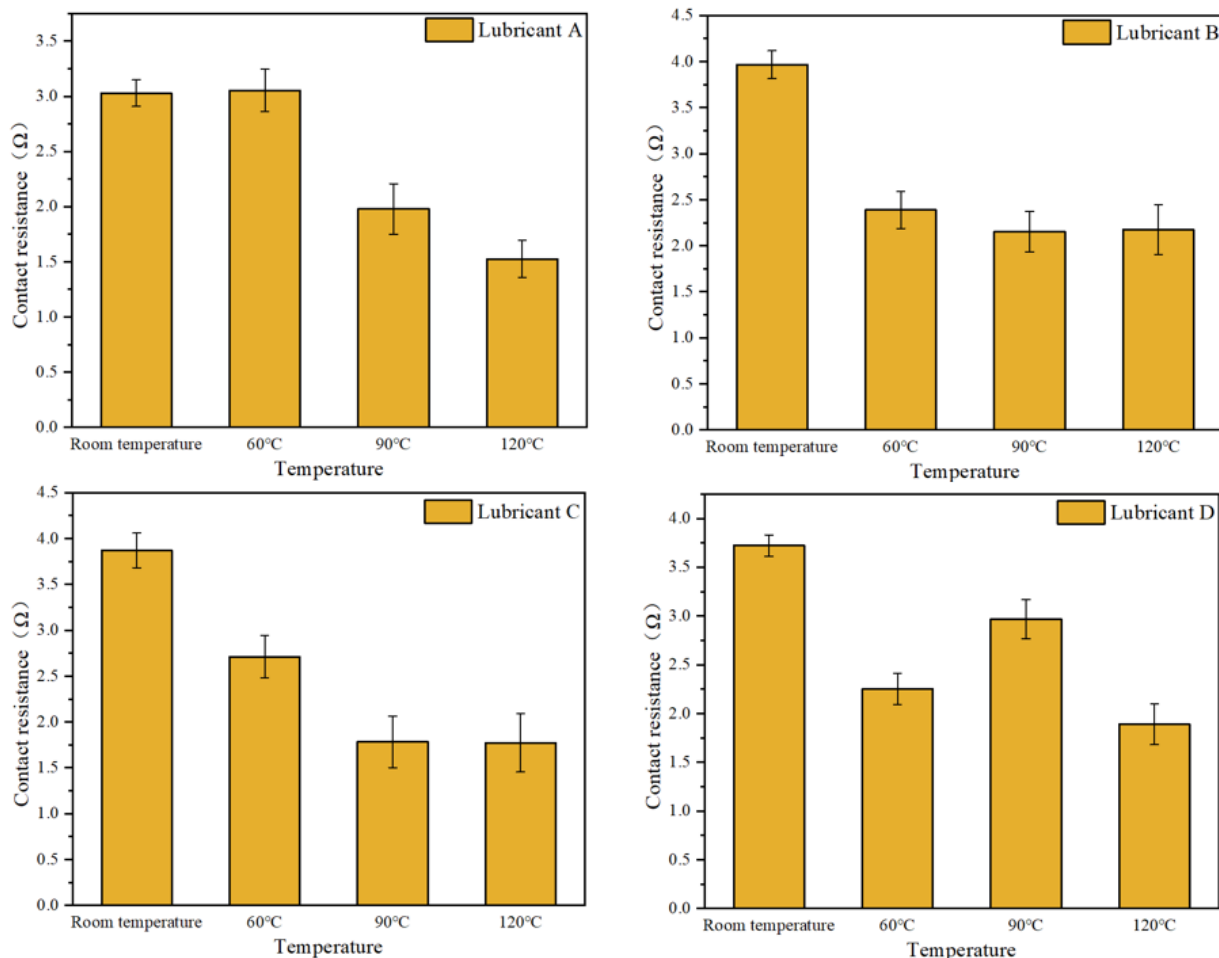


Figure 8. The average contact resistance of the four temperatures.

Table 4. The average contact resistance of the four temperatures.

	Lubricant A	Lubricant B	Lubricant C	Lubricant D
Room temperature	3.0276	3.9668	3.8707	3.7219
60 °C	3.0537	2.3886	2.7117	2.2516
90 °C	1.9795	2.1521	1.783	2.9667
120 °C	1.5261	2.1747	1.773	1.8889

Similar to the results for friction coefficient, lubricating oils B, C, and D showed different change rules to base oil A. The contact resistance showed a trend of decreasing with the increase in temperature, and the contact resistance of the three oils was at the maximum value at room temperature, indicating that the three lubricating oils were in a good lubrication state at room temperature, which was also the reason why the friction coefficient was at the minimum value at room temperature. It should be explained that

the contact resistance of lubricating oil D increased at 90 °C, showing that the thickness of the lubricating-oil film at this temperature was larger than at 60 °C and 120 °C. Combined with the analysis of the change trend in Figure 7, the friction coefficient of lubricating oil D fluctuated less at 90 °C and was more stable than that at 60 °C, reflecting the fact that the friction state of lubricating oil D was relatively stable at 90 °C, the state of the lubricating oil was good, and the lubricating-oil film was stable. For lubricating oil B, the contact resistance did not show a significant difference at high temperatures, which is consistent with the result of the average friction coefficient. As the temperature continued to rise, the lubrication state of the friction pair did not decrease significantly, and it was kept stable within the temperature range of 60 °C to 120 °C. The contact resistance of the four lubricating oils reached the minimum value at 120 °C, the viscosity decreased with the increase in temperature, the film-forming ability of the lubricating oils decreased, and the temperature increase reduced the lubrication characteristics of the lubricating oils. Compared with the base oil A, the viscosity of the lubricating oils B, C, and D was larger, and the influence of the temperature rise on the lubrication characteristics of the friction pair all showed an inhibition effect under test conditions.

3.3. Surface Topography

The surface-roughness evaluation of the material included a variety of characteristic parameters. Two typical parameter were selected in this paper, namely 3D roughness (S_q) and the valley liquid retention index (S_{vi}). S_q reflects the roughness of the friction surface, as the larger the value of S_q , the rougher the surface. S_{vi} reflects the ability of the surface to store liquid: the larger the value of S_{vi} , the stronger the ability of the surface to store liquid.

The surface-characteristic-parameter result for the four lubricating oils at different temperatures is shown in Figure 9 and Table 5, and the surface topography is shown in Table 6; the result of the surface topography was consistent with the analysis results of contact resistance and friction coefficient. The S_q value of base oil A decreased first and then increased with the increase in temperature, while the S_{vi} value also increased first and then decreased, which was consistent with the change trend of the friction coefficient. With the increase in temperature, the surface roughness of base oil A after friction first decreased and then increased, and reached the maximum value at 120 °C. Combined with the analysis of the friction coefficient and contact resistance, the optimum operating temperature of base oil A was 60 °C; the frictional interface had the best frictional performance and achieved good lubrication. While at 120 °C the frictional performance was worse, the temperature seriously affected the lubrication performance of the lubricating oil at 120 °C. The lubricating-oil evaporation and viscosity decrease led to the decrease in the lubricating-oil-film thickness. In addition, a small amount of lubricating-oil carbonization and mixing with grinding chips in the friction pair also aggravated the wear.

Table 5. The average contact resistance of the four temperatures.

	Lubricant A		Lubricant B		Lubricant C		Lubricant D	
	S_q	S_{vi}	S_q	S_{vi}	S_q	S_{vi}	S_q	S_{vi}
Room temperature	1.635	2.413	1.769	3.138	1.203	3.301	1.233	3.205
60 °C	1.102	3.763	2.195	2.332	1.681	2.784	1.537	2.178
90 °C	1.836	3.086	2.253	2.156	1.429	2.103	1.799	2.086
120 °C	2.673	1.532	2.517	1.938	1.932	2.28	1.866	2.173

Similar to the variation law of the friction coefficient and contact resistance, the surface-characteristic parameters of lubricating oils B, C, and D all showed different variation trends to base oil A. With the increase in temperature, the S_q values of the three lubricating oils all showed an increasing trend, while the S_{vi} values showed a decreasing trend, which was consistent with the analysis results for contact resistance and friction coefficient. At room temperature, the S_{vi} of lubricating oils B, C, and D reached the maximum value, which indicated that the lubrication state at room temperature was best. Therefore, the

friction coefficient of the three lubricating oils at room temperature was at the lowest value. Compared with room temperature, the value of S_{vi} at 60 °C decreased, and the increase in temperature reduced the lubrication state of the friction pair of the three lubricating oils. However, with the continued rise in temperature, S_{vi} remained at a relatively stable level within the test temperature range, which was the same as the friction-coefficient trend. Compared with room temperature, the S_q values of lubricating oils B, C, and D were the largest at 120 °C, which was similar to the S_q result for base oil A. The friction and wear on the sample surface were intensified with the temperature increase, which can also be seen from the three-dimensional topography of the friction-pair surface. As the temperature increased, scratches and friction wear on the surface of the sample were intensified, and the surface wear of lubricating oils B, C, and D was the least at room temperature. As the temperature increased, the wear of the sample was intensified, which was consistent with the change rule of S_q .

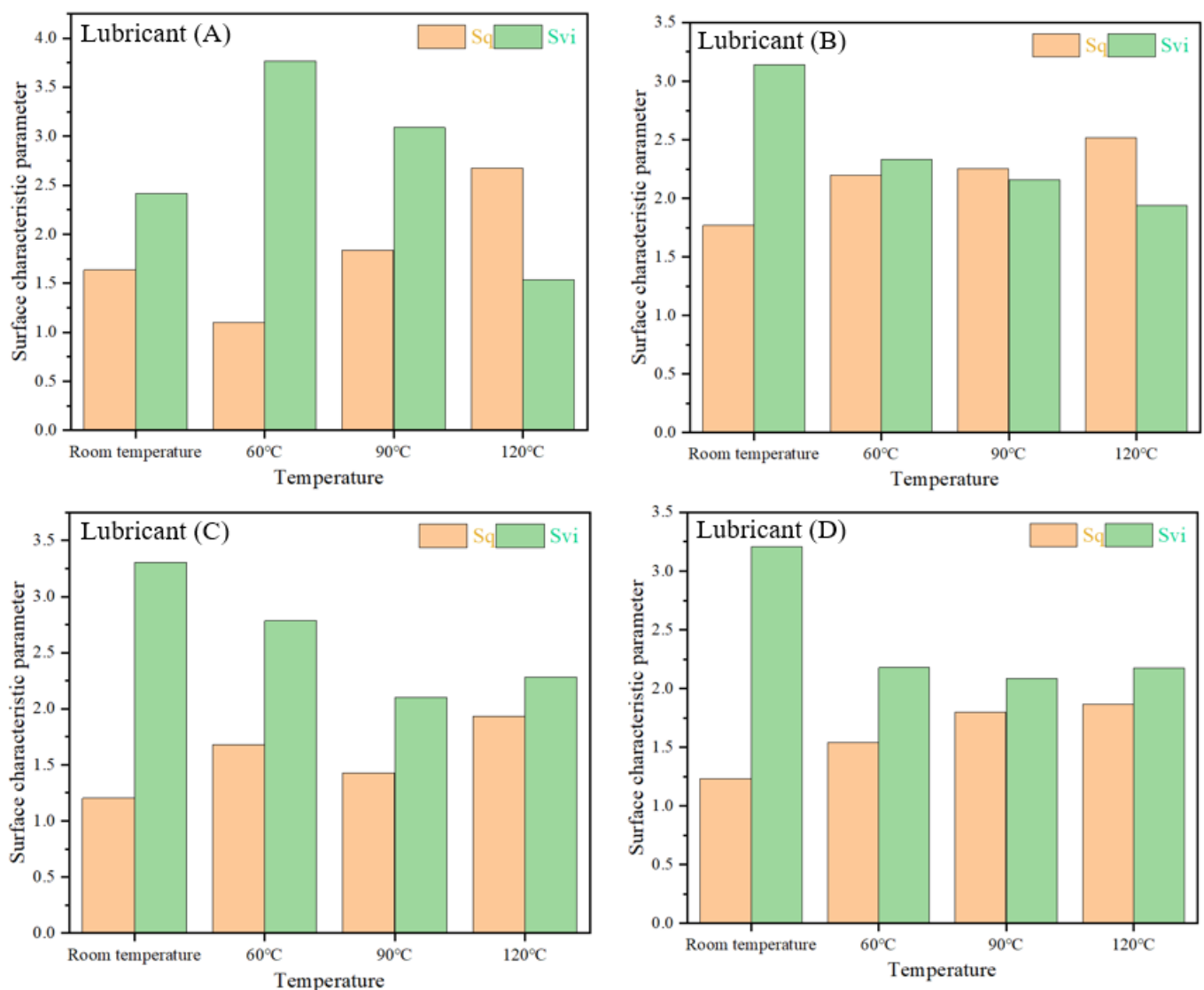
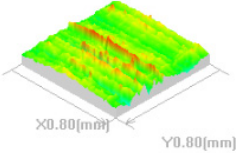
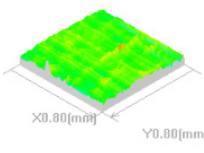
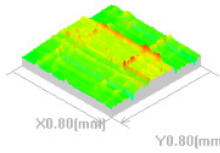
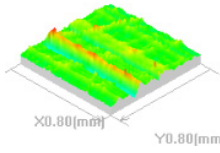
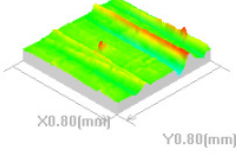
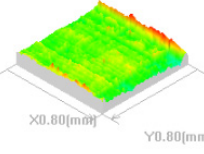
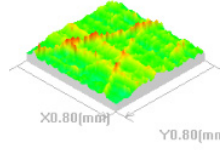
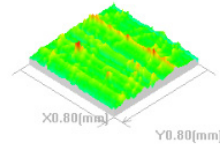
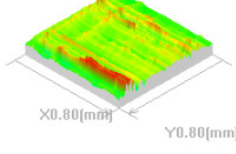
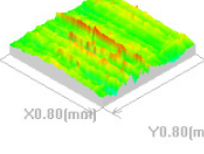
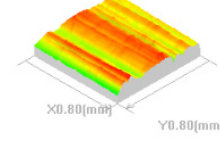
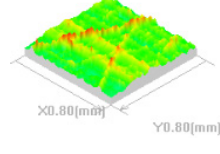
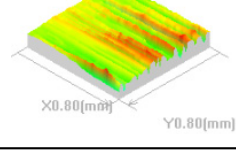
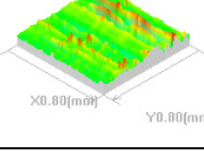
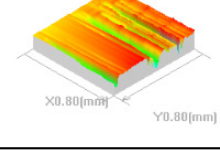
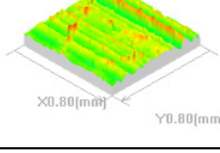


Figure 9. The average contact resistance of the four temperatures.

3.4. SEM Surface Analysis

In order to further analyze the wear of the friction pairs at different temperatures, we selected the samples of lubricating oil D after testing at four temperatures, and their microscopic surfaces were photographed using a scanning electron microscope. The surface morphology of the samples at different temperatures is shown in Figure 10.

Table 6. Surface 3D morphologies of different lubricating oil samples.

Temperature	Lubricant A	Lubricant B	Lubricant C	Lubricant D
Room temperature				
60 °C				
90 °C				
120 °C				

From Figure 10a, we can see that there were many wear marks and slight spalling on the surface of the sample, and fine wear chips can be observed in the wear marks. In the friction process, the micro-convex surface of the sample was worn off to form grinding chips, and became hardened under the reciprocating rolling of the friction pair. With the reciprocating scraping of the CL-PR, obvious furrows formed on the surface of the cylinder liner. In addition, as the test progressed, and the sample surface was fatigued with wear, there was a shallow-spalling phenomenon. Compared with room temperature, the surface wear of the sample was further aggravated at 60 °C, and a large area of irregular pits were observed on the surface of the cylinder liner. This was because the friction heat accumulated irregularly on the surface of the sample as the temperature rose, and aggravated the wear.

As the temperature continued to rise, as can be seen in Figure 10c, scratches increased on the surface of the sample, and more fine, abrasive chips could be observed, which were due to typical abrasive wear [26]. Compared with the surface microstructure at 60 °C, the scratches increased and the abrasive wear was aggravated at 90 °C. While the temperature was at 120 °C, scaly adhesive was observed on the sample surface, which was due to the friction between the CL-PR; the sample surface was torn, resulting in the production of the adhesive, and large scratches were observed on the sample surface, which were caused by abrasive wear. There were also many fine abrasive grains in the furrows. This indicated that, with the increase in temperature, the wear form of the friction pair changed, and adhesive wear occurred on the sample surface at a high temperature. The main wear forms were adhesive wear and abrasive wear. From Figure 10, consistent with the analysis results of the friction coefficient and contact resistance, the friction and wear of CL-PR increased with the increase in temperature.

In addition, to further analyze the reason for the variation in the friction coefficient of base oil A with increasing temperature, an EDS spectrometer (EDS, Oxford, UK) was used to conduct an element analysis on the sample surface. Samples with base oil A at different temperatures were selected for analysis, and the analysis results are shown in Table 7. The distribution of Fe and O elements on the sample surface is shown in Figure 11.

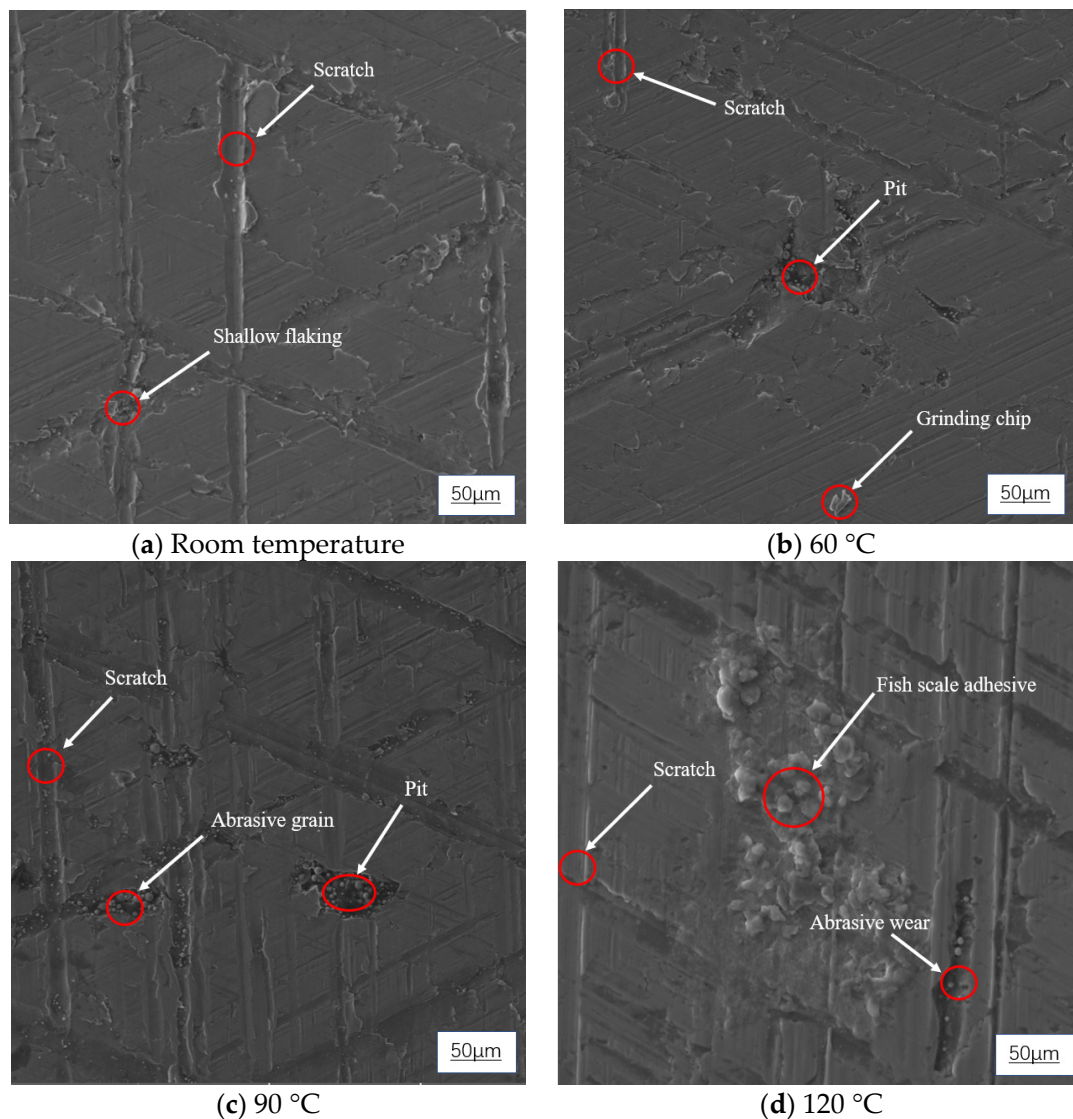


Figure 10. (a) Surface morphology of lubricating-oil-D samples at room temperature; (b) surface morphology of lubricating-oil-D samples at 60 °C; (c) surface morphology of lubricating-oil-D samples at 90 °C; (d) surface morphology of lubricating-oil-D samples at 120 °C.

Table 7. Content of elements on the surface of samples of base oil A.

	Fe Percentage	Si Percentage	O Percentage	C Percentage
Room temperature	96.64%	2.1%	1.26%	0%
60 °C	91.51%	1.8%	6.69%	0%
90 °C	85.9%	4.73%	9.38%	0%
120 °C	79.65%	3.1%	11.15%	6.1%

As can be seen from Table 4, the percentage content of element O shows a strong correlation with the temperature. With the increase in temperature, the content of the element oxygen gradually increased, which shows that the temperature rise promoted the formation of the oxide film [27,28]. The higher the temperature, the more likely it was that the metal oxidation reaction occurred at the friction interface, and formed hard oxide film to protect the friction surface. This was also an important reason why the friction coefficient of base oil A showed a decreasing trend at 60 °C. In addition, element C was observed on the surface of the friction pair at 120 °C, which was consistent with the experimental observation result. There was a carbonization phenomenon of base oil A at 120 °C, which

led to the deterioration of the friction property of base oil A at 120 °C, and increased the friction coefficient.

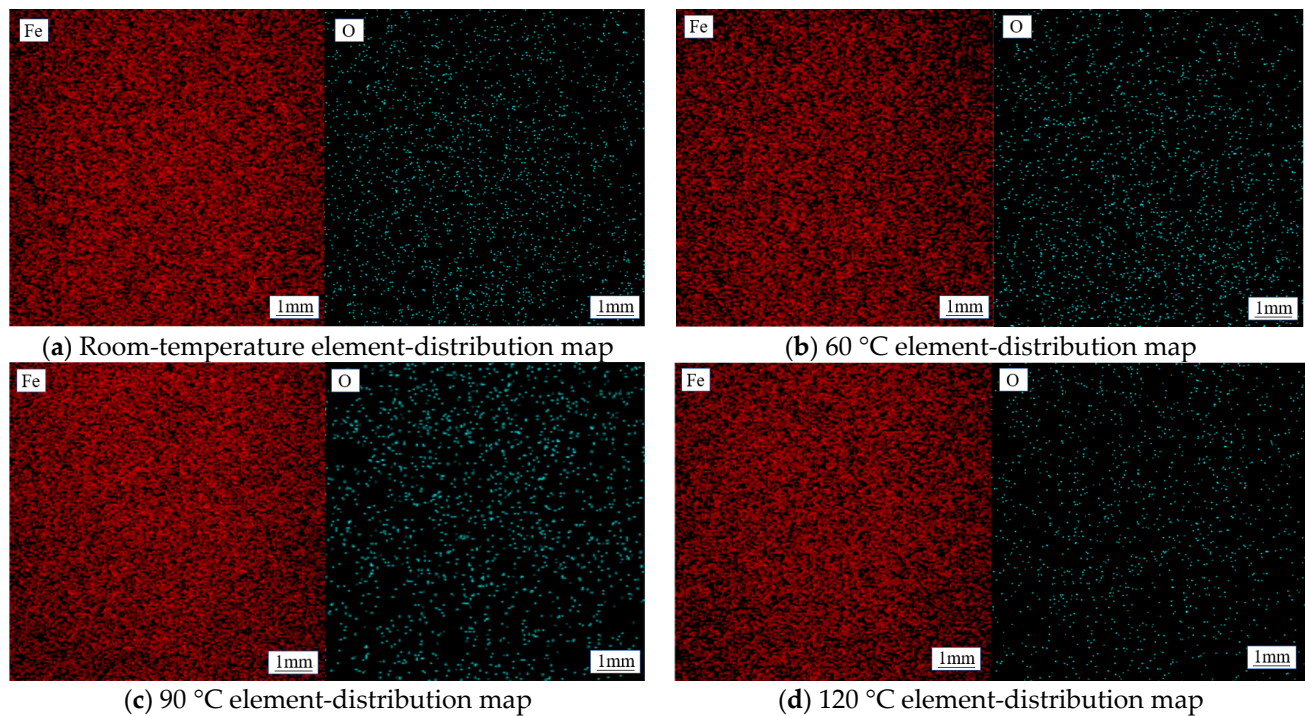


Figure 11. (a) Sample-surface element distribution of lubricant A at room temperature; (b) sample-surface element distribution of lubricant A at 60 °C; (c) sample-surface element distribution of lubricant A at 90 °C; (d) sample-surface element distribution of lubricant A at 120 °C.

4. Discussion

In order to analyze the influence of temperature and lubricating oil on the friction performance of CL-PR, the friction and wear characteristics of the friction pair under different working conditions were analyzed from the three aspects of friction coefficient, contact resistance and surface topography, by controlling the test temperature of the friction-reciprocating-testing machine.

The results showed that the four lubricating oils show different change trends in friction properties with the increase in temperature. The friction coefficient of base oil A decreased first and then increased with the increase in temperature, while the friction coefficient of lubricating oils B, C, and D increased first and then remained stable with the increase in temperature. For base oil, with low viscosity, although the increase in temperature decreased the viscosity of the lubricating oil, the influence of temperature on the friction interface still improved the friction performance of the friction pair, and the wettability of the friction-pair interface was improved [29–31]. During the test, it was observed that the distribution of lubricating oil between the friction pairs changed with the increase in temperature, as shown in Figure 12. Due to the increase in temperature, the wettability of the metal surface was enhanced, and the distribution of lubricating oil on the surface of the friction pair was more uniform. This was also conducive to the formation of more continuous lubricating-oil film and the improvement in the lubrication state of the friction pairs. With the increase in temperature, the metal surface was easy to oxidize. The hard oxide film generated alleviated the friction between the friction pairs and protected the friction surface. At 120 °C, the friction properties of the metal at the friction interface changed, and the friction surface was more likely to wear; the wear forms were abrasive wear and adhesive wear. Compared with other temperature conditions, the wear at 120 °C was more serious. On the other hand, the lubricating property of the base oil was greatly affected at high temperature, the film-forming ability was reduced, and the deterioration of

the oil directly affected the lubrication performance of the CL-PR. Therefore, the friction performance of CL-PR deteriorated at 120 °C, and the friction coefficient was the highest at 120 °C.

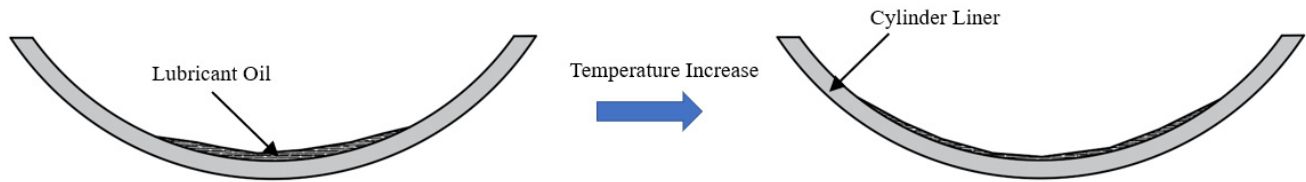


Figure 12. Diagram of the influence of temperature on the distribution of lubricating oil during the test.

The friction coefficient of the lubricating oils B, C, and D increased first and then remained stable with the increase in temperature. From Figure 2, we can see that the viscosity of the lubricating oils B, C, and D decreased significantly with the increase in temperature, and while the viscosity of the base oil was relatively small at room temperature, the decrease was much smaller than that of the other three lubricating oils, which was an important reason why the tribological properties of the base oil showed a different trend to the other three lubricating oils. As the temperature rose, the viscosity of the lubricating oil decreased, and this greatly affected the lubrication performance of the lubricating oil and reduced the thickness of the lubricating oil, which could also be seen from the contact-resistance value of the lubricating oils B, C, and D. Therefore, compared with room temperature, the friction coefficients of the three lubricating oils showed an upward trend at 60 °C, while with the continued rise in temperature, the viscosity was not significantly affected by temperature at 60–120 °C. The situation in Figure 12 was also observed during the test of the lubricating oils B, C, and D, and was an important reason why the friction coefficient remained stable at 60–120 °C.

For LNG engines, temperature not only affects the tribological properties of the CL-PR, but also increases NO_x emissions, due to high temperature under high-power operating conditions [32,33]. Therefore, the control of the running temperature of the cylinder liner and piston ring can be considered a reliable means for improving the comprehensive performance of LNG diesel engines in the future.

5. Conclusions

The influence of temperature and lubricating oil on the friction performance of CL-PR was studied under test conditions, and the influence of the lubricating oil on friction performance was compared at different temperature by analyzing the friction coefficient, contact resistance and surface morphology. The conclusions are as follows:

For base oil A, the friction coefficient decreases first and then increases, and reaches the maximum value at 120 °C. The specific degree of temperature rise promotes the formation of the oxide film, and improves the friction properties of the friction pair; the carbonization of the lubricating oil at 120 °C is one of the reasons for the deterioration of the friction properties of the lubricating oil.

For lubricating oils B, C, and D, under specific application scenarios, the decrease in lubricating-oil viscosity was the main reason leading to the decrease in friction property of the friction pair at room temperature, ~60 °C. While at 60–120 °C the viscosity was not significantly affected by temperature, the lubricating properties of the lubricating oil did not decrease significantly, and the friction coefficient remained stable.

The results of the morphology analysis were consistent with the friction coefficient. The wear of the friction specimen surface was enhanced at a high temperature. With the increase in temperature, the surface-wear forms of the sample changed into abrasive wear and fatigue wear at 120 °C.

Author Contributions: C.D.: methodology, data curation, formal analysis, writing—original draft preparation. C.S.: conceptualization, funding acquisition. X.L.: formal analysis. X.R.: formal analysis. Z.G.: methodology, validation, writing—reviewing and editing. All authors have read and agreed to the published version of the manuscript.

Funding: This research was funded by National Science Foundation of China-Zhejiang Joint Fund for the Integration of Industrialization and Informatization (Grant No. U1709215).

Data Availability Statement: The raw/processed data required to reproduce these findings cannot be shared at this time, as the data also form part of an ongoing study. Meanwhile, raw/processed data will be made available upon request.

Conflicts of Interest: The authors declare that they have no known competing financial interests or personal relationships that could have appeared to influence the work reported in this paper.

References

- Pan, P.C.; Sun, Y.W.; Yuan, C.Q.; Yan, X.P.; Tang, X.J. Research progress on ship power systems integrated with new energy sources: A review. *Renew. Sustain. Energy Rev.* **2021**, *144*, 111048. [\[CrossRef\]](#)
- Cetin, O.; Sogut, M.Z. A new strategic approach of energy management onboard ships supported by exergy and economic criteria: A case study of a cargo ship. *Ocean. Eng.* **2021**, *219*, 108137. [\[CrossRef\]](#)
- Zhu, Y.Q.; Zhou, S.; Feng, Y.M.; Hu, Z.K.; Yuan, L. Influences of solar energy on the energy efficiency design index for new building ships. *Int. J. Hydrogen Energy* **2017**, *42*, 19389–19394. [\[CrossRef\]](#)
- Sahoo, P.; Das, S.K. Tribological Materials—An Ecosustainable Perspective. In *Progress in Green Tribology: Green and Conventional Techniques*; Davim, J.P., Ed.; GER-De Gruyter: Berlin, Germany, 2017; pp. 1–38.
- Satish, K.; Hyoun, T.K.; Kwang, H.C.; Wonsub, L.; Jae, H.C.; Kyungjae, T.; Moon, I. LNG: An eco-friendly cryogenic fuel for sustainable development. *Appl. Energy* **2011**, *88*, 4264–4273.
- Wang, S.J. A portrait of the future of a new generation of LNG fuel ships. *China Ship Surv.* **2022**, *3*, 66–70. (In Chinese)
- Nadiri, S.; Agarwal, S.; He, X.Y.; Kuehne, U.; Fernandes, R.; Shu, B. Development of the chemical kinetic mechanism and modeling study on the ignition delay of liquefied natural gas (LNG) at intermediate to high temperatures and high pressures. *Fuel* **2021**, *302*, 121137. [\[CrossRef\]](#)
- Yan, X.L.; Ge, S.L.; Zun, H.Z.; Jun, J.L. Application of reformed exhaust gas recirculation on marine LNG engines for NO_x emission control. *Fuel* **2021**, *291*, 120114.
- Zhen, L.; Meng, H.M.; Tian, Y.W.; Tian, L.L.; Huai, Y.W.; Yi, Z.F.; Lei, S. Numerical research of the in-cylinder natural gas stratification in a natural gas-diesel dual-fuel marine engine. *Fuel* **2023**, *337*, 126861.
- Li, R.; Wen, C.W.; Meng, X.H.; Xie, Y.B. Measurement of the friction force of sliding friction pairs in low-speed marine diesel engines and comparison with numerical simulation. *Appl. Ocean. Res.* **2022**, *121*, 103089. [\[CrossRef\]](#)
- Delprete, C.; Razavykia, A. Piston ring-liner lubrication and tribological performance evaluation: A review. *Eng. Tribol.* **2017**, *232*, 193–209. [\[CrossRef\]](#)
- Forder, M.D.; Morris, N.; King, P.; Balakrishnan, S.; Howell, S.S. An experimental investigation of low viscosity lubricants on three piece oil control rings cylinder liner friction. *Proc. IMechE Part J. Eng. Tribol.* **2022**, *236*, 2261–2271. [\[CrossRef\]](#)
- Rahmani, R.; Rahnejat, H.; Fitzsimons, B.; Dowson, D. The effect of cylinder liner operating temperature on frictional loss and engine emissions in piston ring conjunction. *Appl. Energy* **2017**, *191*, 568–581. [\[CrossRef\]](#)
- Daniel, S.G.; Samuel, L.; Ashlie, M. Effect of Temperature and Surface Roughness on the Tribological behavior of electric motor greases for hybrid bearing materials. *Lubricants* **2021**, *9*, 59.
- Ze, Q.L.; Ming, L.X.; Hong, H.Z.; Wei, F.H.; Guang, A.Z.; Zhi, B.L. Effect of silicon-doping on the wide-temperature tribological behavior and lubrication mechanism of WC/a-C film. *Wear* **2023**, *516–517*, 204614.
- Jiménez, A.; Bermúdez, M. Friction and Wear. In *Tribology for Engineers: A Practical Guide*; Davim, J., Ed.; Elsevier: Amsterdam, The Netherlands, 2011; pp. 33–63.
- Zhen, B.C.; Yan, Z.; Jun, Q. Effect of oil temperature on tribological behavior of a lubricated steel–steel contact. *Wear* **2015**, *332–333*, 1158–1163.
- Peter, S.; Khaled, G.; Simo, P.; Guillaume, C.; Tobin, F. High temperature microtribological studies of MoS₂ lubrication for low earth orbit. *Lubricants* **2020**, *8*, 49.
- Yi, C.X.; Akihiko, Y.; Noriyuki, H.; Norihisa, H.; Guo, X.X.; Dan, G. Analysis of temperature and heat partitioning coefficient during friction between polymer and steel. *Tribol. Int.* **2022**, *171*, 107561.
- Sepehr, S.; Farnaz, B.; Andreas, A.P.; Ali, B. Elevated temperature contact creep and friction of nickel-based superalloys using machine learning assisted finite element analysis. *Mech. Mater.* **2022**, *171*, 104346.
- Ye, L.X.; Yu, C.; Ming, X.S.; Ping, P.Y.; Jun, H.D.; De, H.J.; Huo, P.Z.; Shao, P.L.; Li, C.H. Friction and wear behavior of copper metal matrix composites at temperatures up to 800 °C. *J. Mater. Res. Technol.* **2022**, *19*, 2050–2062.
- Caglar, D.; Cengiz, D. Effect analysis on energy efficiency enhancement of controlled cylinder liner temperatures in marine diesel engines with model based approach. *Energy Convers. Manag.* **2020**, *220*, 113015.

23. Hubert, K.; Mirosław, J.; Artur, J.; Janusz, L.; Krzysztof, B. Effect of temperature on tribological properties of 1-butanol-diesel fuel blends-Preliminary experimental study using the HFRR method. *Fuel* **2021**, *296*, 120700.
24. Geng, Z.; Li, S.; Duan, D.L.; Liu, Y. Wear behaviour of WC–Co HVOF coatings at different temperatures in air and argon. *Wear* **2015**, *330–331*, 348–353. [[CrossRef](#)]
25. Jing, W.; Peng, G.; Hao, L.; Pei, L.K.; Ai, Y.E. Insights on high temperature friction mechanism of multilayer ta-C films. *J. Mater. Sci. Technol.* **2022**, *97*, 29–37.
26. Ryu, T.; Shrotriya, P. Wear and Corrosion Damage of Medical-Grade Metals and Alloys. In *Wear of Advanced Materials*; Davim, J., Ed.; Wiley: London, UK, 2013; pp. 164–193.
27. Vijay, K.; Debarati, B. Comparison of quantitative elemental depth distribution analyses of Ni and Ti in co-sputtered Ni-Ti alloy thin films using MCs⁺ and M⁺ secondary ions. *Thin Solid Film.* **2022**, *753*, 139292.
28. Hari, S.B.; Subhashis, B.; Amit, K.K.; Indranil, S.; Sandeep, P.; Sanjit, S.; Prasenjit, M. Tuned synthesis and designed characterization of graphene oxide thin film. *Inorg. Chem. Commun.* **2022**, *139*, 109356.
29. Chun, L.; Xin, C.J.; Xiao, T.C.; Ji, L.M. Experimental study on the evolution of friction and wear behaviours of railway friction block during temperature rise under extreme braking conditions. *Eng. Fail. Anal.* **2022**, *141*, 106621.
30. Xin, Y.L.; Yue, J.; Zhong, H.J.; Yun, C.L.; Cuie, W.; Jian, S.L. Reversible wettability transition between superhydrophilicity and superhydrophobicity through alternate heating-reheating cycle on laser-ablated brass surface. *Appl. Surf. Sci.* **2019**, *492*, 349–361.
31. Chi, V.N.; Doo, M.C. Fast wettability transition from hydrophilic to superhydrophobic laser-textured stainless steel surfaces under low-temperature annealing. *Appl. Surf. Sci.* **2017**, *409*, 232–240.
32. Zheng, F.; Zhang, H.F.; Yin, H.; Fu, M.L.; Jiang, H.; Li, J.Q.; Ding, Y. Evaluation of real-world emissions of China V heavy-duty vehicles fueled by diesel, CNG and LNG on various road types. *Chemosphere* **2022**, *303*, 135137. [[CrossRef](#)] [[PubMed](#)]
33. Zhang, C.H.; Zhou, A.; Shen, Y.C.; Li, Y.Y.; Shi, Q. Effects of combustion duration characteristic on the brake thermal efficiency and NO_x emission of a turbocharged diesel engine fueled with diesel-LNG dual-fuel. *Appl. Therm. Eng.* **2017**, *127*, 312–318. [[CrossRef](#)]

Disclaimer/Publisher's Note: The statements, opinions and data contained in all publications are solely those of the individual author(s) and contributor(s) and not of MDPI and/or the editor(s). MDPI and/or the editor(s) disclaim responsibility for any injury to people or property resulting from any ideas, methods, instructions or products referred to in the content.